Lithos 338–339 (2019) 87–98

Contents lists available at ScienceDirect

Lithos

journal homepage: www.elsevier.com/locate/lithos

Olivine O isotope and trace element constraints on source variation of picrites in the Emeishan flood basalt province, SW China

Jun-Hua Yao [a,b], Wei-Guang Zhu [a,*], Chusi Li [a,c], Hong Zhong [a,b], Songyue Yu [a], Edward M. Ripley [c], Zhong-Jie Bai [a]

[a] State Key Laboratory of Ore Deposit Geochemistry, Institute of Geochemistry, Chinese Academy of Sciences, Guiyang 550081, China
[b] University of Chinese Academy of Sciences, Beijing 100049, China
[c] Department of Earth and Atmospheric Sciences, Indiana University, Bloomington, IN 47405, USA

ARTICLE INFO

Article history:
Received 10 December 2018
Accepted 22 April 2019
Available online 24 April 2019

Keywords:
Olivine O isotopes
Olivine trace element ratios
Mantle plume heterogeneity
Picrites
Continental flood basalts
SW China

ABSTRACT

Like many continental flood basalt (CFB) provinces in the world, the source mantle compositions (peridotites or pyroxenites) of the Emeishan CFB province in SW China are still debated. We have used the combination of olivine O isotopes determined in situ using SIMS and trace element abundances measured in situ using LA-ICP-MS to address this fundamental problem. The newly discovered picrites in the Emeishan CFB province at Yumen are used in this study. In addition, we have also analyzed primitive olivine phenocrysts with known O isotope ratios from four other picrite occurrences (Maoniuping, Tanglanghe, Wuguijing and Wulongba) in the Emeishan CFB province for trace element abundances. Based on whole rock compositions the picrite samples from Wulongba belong to the low-Ti group (Ti/Y < 500) and those from the other locations belong to the high-Ti group (Ti/Y > 500). Mineral chemical data reveal that the two different groups of picrites can be distinguished by using Ti/Al of olivine phenocrysts and Cr-spinel inclusions enclosed in olivine. Specifically, the high-Ti picrite group is characterized by 10Ti/Al (molar) >0.9 and >0.5 for olivine phenocrysts and Cr-spinel inclusions, respectively. In the mantle source discrimination diagrams based on olivine 100Mn/Fe versus 100Ni/Mg or 100Ca/Fe, both groups of picrites plot between the suggested fields of peridotite and pyroxenite mantle sources. In the same type of diagrams based on olivine Mn/Zn and 10000Zn/Fe, both groups of picrites plot exclusively in the fields for a peridotite mantle source. The mean $\delta^{18}O$ value of olivine phenocrysts from the Yumen high-Ti picrites is 5.19 ± 0.25‰ (1σ, $n = 35$), which is significantly lower than that for the Wulongba low-Ti picrites (5.6 ± 0.15‰) but is similar to values (5.1 ± 0.15 to 5.3 ± 0.15‰) for the high-Ti picrites from elsewhere (Maoniuping, Talanghe and Wuguijing) in the Emeishan CFB province. The mean $\delta^{18}O$ values of olivine phenocrysts from the Emeishan high-Ti picrites at different locations are all within the range of typical mantle olivine values (5.1 ± 0.3‰). Based on these results, we conclude that the high-Ti picrites in the Emeishan CFB province were primarily derived from a modally enriched peridotite mantle source. Our new olivine Zn-Mn-Fe data are consistent with the view that the Wulongba low-Ti picrites were derived from a lithospheric peridotite mantle source.

1. Introduction

It is widely believed that oceanic island basalts (OIB) and continental flood basalts (CFB) are the products of deep-seated mantle plume activity in oceanic and continental settings, respectively (e.g., Campbell and Griffiths, 1990; Morgan, 1971; Richards et al., 1989). These lavas were used by some researchers to study the chemical and lithological heterogeneity of the deep mantle, and the interaction between a mantle plume and the lithosphere (e.g., Ireland et al., 2011; Lassiter and Hauri, 1998). Previous studies of CFB provinces in different parts of the world such as Emeishan, Karoo, Siberia, and West Greenland (e.g., Ali et al., 2005; Arndt et al., 1998; Jourdan et al., 2007; Li et al., 2016; Schaefer et al., 2000; Shellnutt, 2014) have shown that most basalts experienced fractional crystallization as well as crustal contamination. As a result, they are not the best samples to study mantle plume heterogeneity and the involvement of the overlying lithospheric mantle. Minor picrites in some CFB provinces are better samples than the associated basalts for such studies because the picrites generally formed from more primitive magmas plus early-crystallized olivine phenocrysts and are less-contaminated with the crust than the associated basalts (e.g., Larsen and Pedersen, 2009; Starkey et al., 2009; Yu et al., 2017; Zhang et al., 2006a).

In prior studies where picrites have been used to investigate the mantle sources of a CFB province, whole rock geochemical compositions have been employed (e.g., Chung and Jahn, 1995; Ellam, 2006). However, recent studies have demonstrated that in cases such as those of the Emeishan, Karoo, and West Greenland provinces, picrites formed

* Corresponding author.
E-mail address: zhuweiguang@vip.gyig.ac.cn (W.-G. Zhu).

https://doi.org/10.1016/j.lithos.2019.04.019
0024-4937/

by open system instead of closed system processes, and the whole rock data commonly carry mixed signals with respect to magma origin (e.g., Kamenetsky et al., 2012, 2017; Larsen and Pedersen, 2000; Li et al., 2012). The compositions of olivine phenocrysts with low Fo (100 Mg/(Mg + Fe), molar) also can be altered by the crustal contamination. For these reasons many researchers have begun to focus on the geochemical compositions of the most primitive olivine phenocrysts and the melt inclusions trapped in these crystals (e.g., Harris et al., 2015; Jennings et al., 2017; Kamenetsky et al., 2017; Ren et al., 2017).

In the case of the Emeishan CFB province in SW China some researchers (Hanski et al., 2010; Kamenetsky et al., 2012; Ren et al., 2017) have determined the chemical and Pb-isotope compositions of melt inclusions entrapped in the most primitive olivine phenocrysts of the picrites and used the data to evaluate the mantle source compositions. Yu et al. (2017) were the first to use the O isotope ratios of the most primitive olivine phenocrysts in the Emeishan picrites in several areas (Maoniuping, Tanglanghe, Wuguijing and Wulongba) for the same purpose. All of these studies also used the concentrations of several trace elements such as Ni, Mn and Ca in the olivine phenocrysts of the selected picrites as additional constraints. Recently, some researchers have successfully used 10000Zn/Fe and Mn/Zn in primitive olivine to evaluate the mantle source compositions of ultramafic rocks elsewhere in the world (e.g., Le Roux et al., 2010; Howarth and Harris, 2017). This new approach has never been applied to the Emeishan picrites anywhere due to absence of Zn data for olivine phenocrysts in these rocks in the previous studies. In this study, we measured the $^{18}O/^{16}O$ ratios of the primitive olivine phenocrysts in a newly-discovered picrite outcrop at Yumen in the Emeishan CFB using SIMS. In addition, the concentrations of Zn plus other complementary trace elements in the olivine crystals from this area and other areas (Maoniuping, Tanglanghe, Wuguijing and Wulongba) were measured using LA-ICP-MS. The new and previous data are used together to evaluate the heterogeneity of the mantle source for the Emeishan plume.

2. Geological background

The Emeishan flood basalt province is located in the western part (>250,000 km^2) of the South China Block from western Sichuan to northern Vietnam (Fig. 1). The South China Block is a Precambrian continental block formed by the amalgamation of the Yangtze Craton in the north and the Cathaysia block in the south during the Late Neoproterozoic (Cawood et al., 2013, and references therein). The western rim of the South China Block is bounded by two Gondwana-derived micro-continental blocks; the Simao block in the south and the Songpan-Ganze block in the north. The assembly of these three blocks took place in the Early Triassic by the subduction of the Paleo-Tethys oceanic plate (Deng et al., 2014, and references therein).

The basement of the Yangtze Craton is composed of Archean crystalline and high-grade metamorphic rocks and its sedimentary cover is composed of post-Archean low-grade metamorphosed sedimentary rocks. Abundant Neoproterozoic intrusive rocks with composition varying from granodiorites to mafic-ultramafic rocks are present in the western margin of the Yangtze Craton (e.g., Li et al., 2002, 2003; Yao et al., 2018; Zhou et al., 2002; Zhu et al., 2008, and references therein).

In addition to voluminous flood basalts with thickness from 2000 to 5000 m, minor picrites with thickness from 10 to 50 m are present in the western part of the Emeishan flood basalt province from Lijiang to Dali (Fig. 2a, e.g., Chung and Jahn, 1995; Xu et al., 2001; Ali et al., 2005; Zhang et al., 2006a, 2006b, 2008; Shellnutt, 2014, and references therein). In these districts the lavas overlie Early-Late Permian limestones and are overlain by Late Triassic to Jurassic clastic sedimentary rocks (He et al., 2003). The zircon U-Pb ages of the associated mafic-intrusions are between 258 and 260 Ma (e.g., Fan et al., 2008; Hou et al., 2013; Shellnutt et al., 2012; Wang et al., 2012; Zhong et al., 2011; Zhong and Zhu, 2006, and references therein). Some of these intrusions host world-class magmatic Fe-Ti-V oxide ore deposits or small magmatic Ni-Cu and Pt-Pd deposits (Fig. 1b, e.g., Zhong et al., 2002; Zhou et al., 2005; Song et al., 2008; Zhang et al., 2009, and references therein).

The geology of the picrite samples from the Maoniuping, Tanglanghe and Wuguijing and Wulongba areas have been described by Yu et al. (2017). These picritic flows with darker color are associated with Emeishan basalts and have experienced different degrees of alteration. A couple of years ago, we found a picrite outcrop in a road cut ~20 km to the northeast of the town of Yumen (Fig. 2a, b). This picrite flow is interbedded within a basaltic volcanic sequence that is underlain and overlain by Permian limestone and Triassic clastic sedimentary rocks, respectively (Fig. 2b, c). The thickness of the volcanic sequence is ~1500 m. It is mainly composed of basalts and basaltic andesites. The thickness of the associated picrite flow is estimated to be ~5 m based on a road-cut exposure (Fig. 3a). The rock types of the volcanic sequence and its stratigraphic position are similar to the Permian flood basalts that occur elsewhere in the Emeishan CFB province.

3. Samples and analytical methods

3.1. Samples

The picrite samples from Maoniuping, Tanglanghe, Wuguijing and Wulongba areas used in this study and Yu et al. (2017) are the same. The detailed descriptions of these samples are given in Yu et al. (2017). Briefly, the modal composition and primary texture of picrites from these four locations are similar, containing ~20–30% olivine and minor augite phenocrysts, with a groundmass of fine-grained pyroxene and plagioclase.

Eight picrite samples were collected from the newly discovered outcrop in the Yumen district (Fig. 3a). These samples all contain abundant olivine phenocrysts with grain sizes varying from 50 μm to 2 mm across, and rare, generally smaller, clinopyroxene phenocrysts. The morphology of olivine phenocrysts varies from euhedral to subhedral. Serpentine alteration is common but restricted to rims and micro-fractures (Fig. 3b). Clinopyroxene phenocrysts are mostly subhedral (Fig. 3c). Some olivine phenocrysts contain several small Cr-spinel inclusions with diameters less than a few tens of microns (Fig. 3d). Large grains of Cr-spinel are attached to some olivine phenocrysts. The groundmass is composed of very fine-grained clinopyroxene, plagioclase and oxides. Two of the least-altered samples (YBYM1307, YBYM1502) were used for mineral separation. The olivine separates from these samples were used for in situ analysis of O isotope ratios and chemical compositions. In order to ensure that all analyzed spots for major elements, trace elements and O isotopes (^{18}O, ^{16}O) were determined on the same locations of olivine grains, we first carefully selected the appropriate areas on the olivine to analyze, and then made measurements in the order of electron probe, SIMS and LA-ICP-MS (Fig. 3e, f).

3.2. Analytical methods

Major element compositions of whole rocks were determined using X-ray fluorescence spectrometry (XRF) at the ALS Chemex Co Ltd., Guangzhou. The analytical precision was better than 5%. Trace elements in whole rocks were analyzed using a Perkin-Elmer Sciex ELAN DRC-e ICP-MS at the State Key Laboratory of Ore Deposit Geochemistry (SKLODG), Institute of Geochemistry, Chinese Academy of Sciences (IGCAS). The powdered samples (50 mg) were dissolved with a HF + HNO_3 mixture in high-pressure Teflon Bombs at ~190 °C for 48 h. Rh was used as an internal standard to monitor signal drift during counting. The analytical precision is generally better than 10%.

The compositions of olivine separates from Yumen picrites and all Cr-spinel inclusions were determined by wavelength dispersive analysis using a JEOL JXA-8230 electron microprobe at the School of Resources and Environmental Engineering, Hefei University of Technology, China. The analytical conditions were 15 kV accelerating voltage, 40 nA beam current, 3–5 μm beam diameter, and 10–20 s

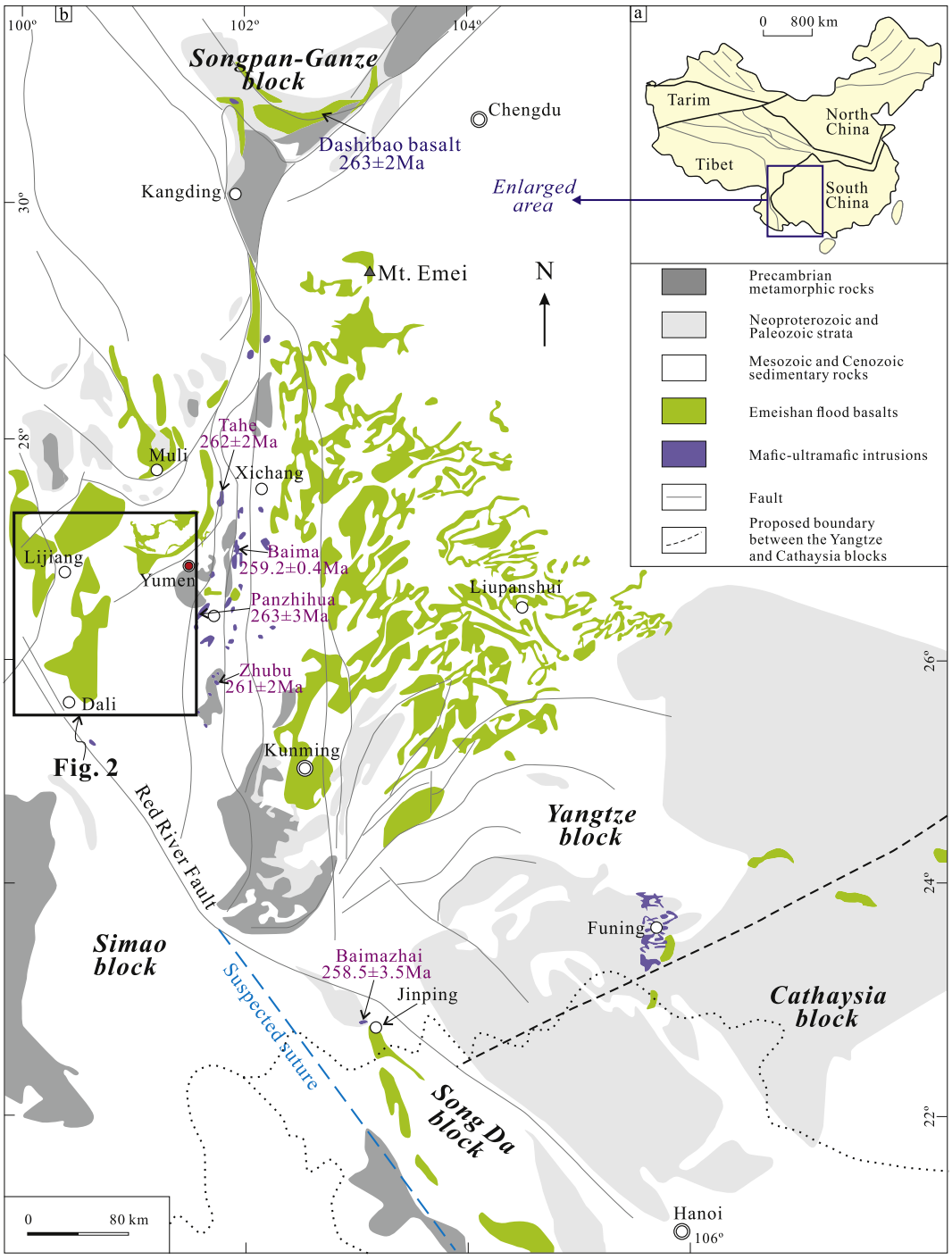

Fig. 1. (a) Schematic map showing the tectonic units of China and (b) distribution of the Emeishan continental flood basalts and coeval mafic-ultramafic intrusions (modified from Li et al., 2016). The suspected suture is from Chung et al. (1997). The zircon U—Pb ages are from Zhou et al. (2005), Wang et al. (2006), Fan et al. (2008) and Shellnutt et al. (2011).

peak counting time. The compositions of olivine phenocrysts from Maoniuping, Tanglanghe and Wuguijing and Wulongba picrites were determined by wavelength dispersive analysis using a JEOL JXA-8530F Plus electron microprobe at the State Key Laboratory of Ore Deposit Geochemistry, Institute of Geochemistry, Chinese Academy of Sciences in Guiyang. The analytical conditions were 25 kV accelerating voltage, 10 nA beam current, 10 μm beam diameter, and 10–20 s peak counting time.

Trace element abundances in olivine were determined by LA-ICP-MS at the State Key Laboratory of Ore Deposit Geochemistry, Institute of Geochemistry, Chinese Academy of Sciences in Guiyang, using a Coherent GeoLasPro 193-nm Laser Ablation system coupled with an Agilent 7900× ICP-MS. Helium (580 ml/min) was applied as a carrier gas. Argon (900 ml/min) was used as the make-up gas and mixed with the carrier gas via a Y-connector before entering the ICP. Ablation protocol employed a spot diameter of 44 μm at 6 Hz with energy of 8 J cm^{-2} fluence. Each analysis incorporated a background acquisition of approximately 30 s (gas blank) followed by 60 s data acquisition from the sample. The Agilent Chemstation was utilized for the acquisition of each individual analysis. ^{29}Si was used as the internal standard. A block of reference materials (NIST SRM 610 and 612, BHVO-2G, BCR-2G and BIR-1G GOR128-G) were used as external standards to plot a calibration curve. Every eight analyses were followed by one analysis of ML3B-G/BCR-2G as quality control of the time-dependent calibration for sensitivity drift.

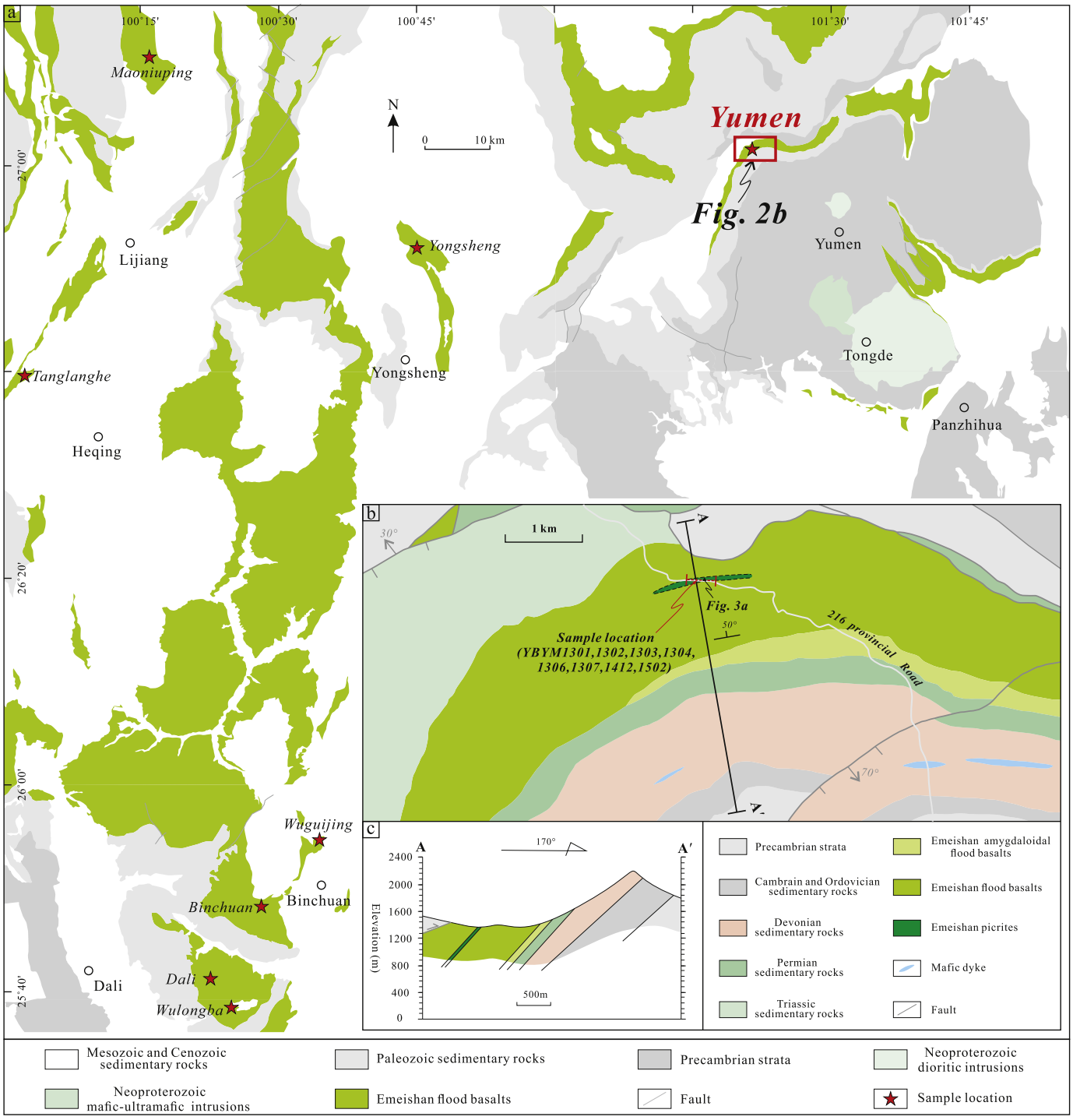

Fig. 2. (a) Distribution of the Emeishan flood basalts and associated picrites in the Dali-Lijiang districts and surrounding areas (modified from Yu et al. (2017). (b) Distribution of Permian basalt-picrite lavas in the Yumen area, with sample locations. (c) Geological cross-section showing the stratigraphic position of the Emeishan flood basalts in Yumen. The sample locations of picrites in the Dali area are from Hanski et al. (2010). The sample locations of picrites in the Binchuan and Yongsheng areas are from Kamenetsky et al. (2012). The sample locations of picrites in the Maoniuping, Tanglanghe, Wuguijing and Wulongba areas are from Yu et al. (2017).

Sc is of particular importance for this study, but ^{45}Sc is affected by interference with $^{29}Si^{16}O$. The concentrations of Sc were calculated from the measured count rate on mass 45 and corrected for interference with $^{29}Si^{16}O^{+}$. A natural Sc-free quartz was measured to calculate the production rate of silica oxide. Off-line selection and integration of background and analytical signals, and time-drift correction and quantitative calibration were performed by ICPMSDataCal (Liu et al., 2008). For other elements except Mg and Fe, the % RSD was better than 10%. Results of replicate measurements of quality control material ML3B-G/BCR-2G (except Mg) agree with their reference values within 10%.

Oxygen isotope ratios of olivine were measured using a CAMECA IMS-1280 ion microprobe in the Institute of Geology and Geophysics, Chinese Academy of Sciences (IGGCAS), Beijing, China. The selected olivine grains from the Yumen picrites and a dozen grains of the San Carlos olivine standard were mounted in epoxy, polished and cleaned.

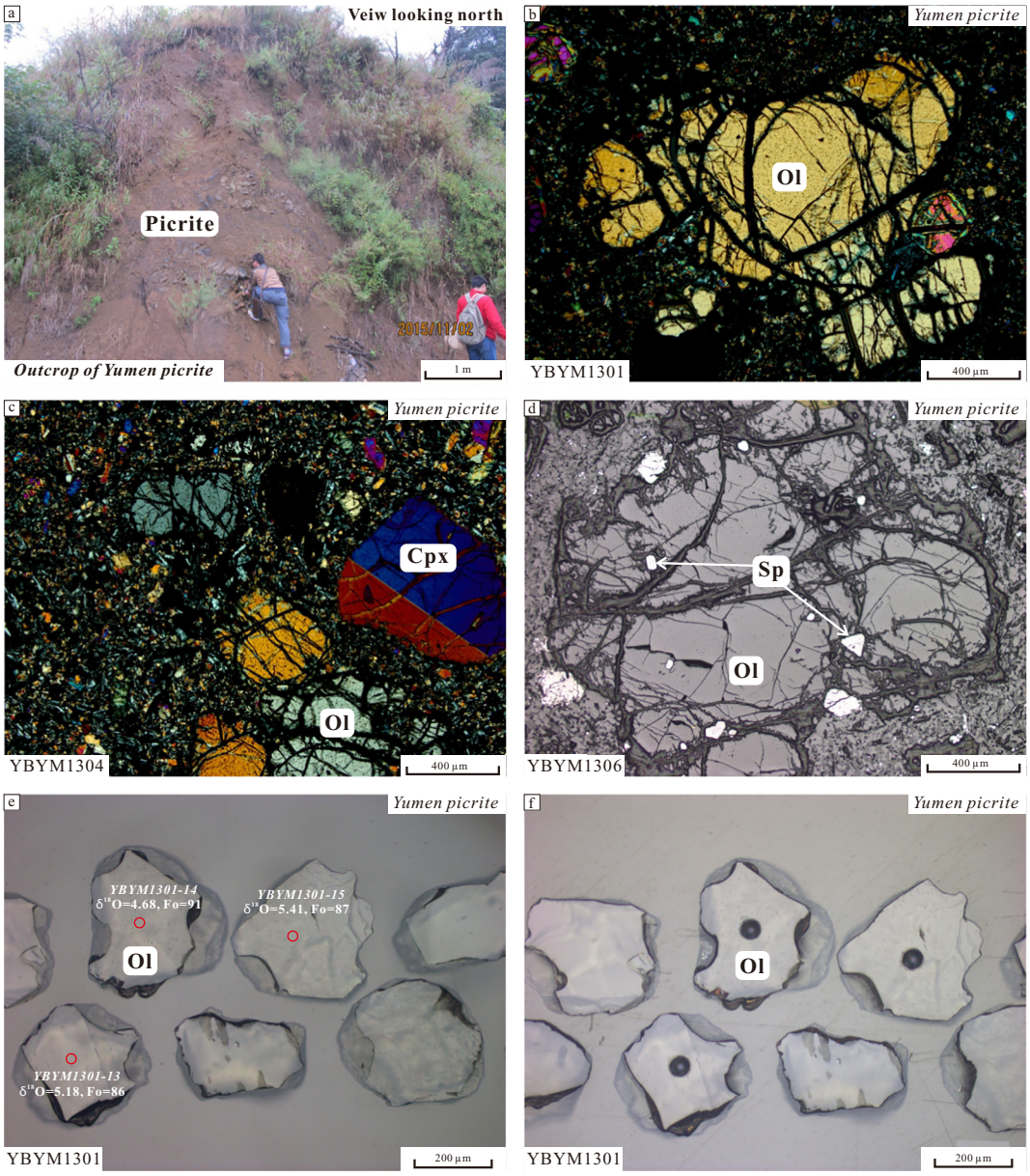

Fig. 3. (a) Outcrop photo of the Yumen basalt-picrite lavas, (b) olivine phenocryst in the picrite, (c) clinopyroxene phenocrysts in the picrite, (d) Cr-spinel inclusions in olivine phenocryst in the picrite. (e) locations of SIMS oxygen isotope analyses in olivine. (f) locations of LA-ICP-MS analyses in olivine. Cpx = clinopyroxene, Ol = olivine, Sp = Cr-spinel.

Target selection was done using reflected light microscopy and back-scattered electron images. A Cs + primary beam was accelerated at 10 kV with an intensity of ca. 2 nA. The spot size was about 10 × 20 μm. An electron gun was used to compensate for sample charging during analysis. Oxygen isotopes (^{18}O, ^{16}O) were measured in multi-collector mode with two off-axis Faraday cups, following the procedures given in Li et al. (2010). The results are presented in standard delta notation: $\delta^{18}O = (({}^{18}O/{}^{16}O)_{sample}/({}^{18}O/{}^{16}O)_{V-SMOW}) - 1$, with conversion to ‰ achieved via multiplication by 1000, where $({}^{18}O/{}^{16}O)_{V-SMOW} = 0.0020052$ (V − SMOW being Vienna Standard Mean Ocean Water). Matrix effects were negligible, within the errors of measurement for olivine with variable Fo from 60 to 100 mol% on a CAMECA IMS 1270/1280 (Bindeman et al., 2008; Eiler et al., 2011; Gurenko et al., 2011). The instrumental drift was corrected using two bracketing standards (San Carlos Olivine Standard with $\delta^{18}O = 5.25‰$, Eiler et al., 1995). The measured results of the San Carlos Olivine Standard during this study are $\delta^{18}O = 5.22‰ \pm 0.25$ (1σ, $n = 15$) (Table A1).

4. Analytical results

4.1. Whole rock chemical compositions

The abundances of major and trace elements in the Emeishan picrites from Yumen are given as supplementary data (Table A2). The picrites from Yumen contain 19.3–20.3 wt% MgO, 1.74–1.89 wt% TiO_2, 13.0–13.4 wt% $Fe_2O_3^{Total}$, with $Mg^{\#}$ (100 Mg/(Mg + Fe^{Total}, molar) of 74 to 75. Their Ti/Y ratios are from 700 to 800, which are significantly higher than the value (500) used to divide the high-Ti and low-Ti basalts in the Emeishan flood basalt province (Xu et al., 2001). Using the combination of whole rock Ti/Y ratios and mantle normalized Gd/Yb ratios, Kamenetsky et al. (2012) classified the Emeishan picrites into high-Ti, low-Ti and intermediate-Ti picrites (Fig. 4a). These authors called the two end-members, Binchuan and Yongsheng, low-Ti and high-Ti picrites, respectively, and all other known occurrences in SW China as intermediate-Ti picrites (Fig. 4a). Clearly, the Emeishan picrites from

Yumen belong to the high-Ti group according to the classification of Xu et al. (2001), but are the members of the intermediate-Ti group according to the classification of Kamenetsky et al. (2012). If the classification of Xu et al. (2001) is adapted, the low-Ti and high-Ti groups of the Emeishan picrites can also be separated using the whole rock TiO_2 content at 1.3 wt% (Fig. 4b).

4.2. Cr-spinel chemical compositions

The chemical compositions of Cr-spinel crystals enclosed in olivine phenocrysts in the Emeishan picrites from Yumen and other localities analyzed by us are given as supplementary data (Table A3). Cr-spinel crystals in the Yumen, Maoniuping, Tanglanghe and Wulongba picrites contain 70–77 $Cr^{\#}$ (100Cr/(Cr + Al), molar) and 33–40 $Mg^{\#}$ (100 Mg/(Mg + Fe^{2+}), molar), 66–73 $Cr^{\#}$ and 35–49 $Mg^{\#}$, 65–76 $Cr^{\#}$ and 34–49 $Mg^{\#}$, 62–71 $Cr^{\#}$ and 46–71 $Mg^{\#}$, respectively. If the classification of Xu et al. (2001) is adapted, the Emeishan low-Ti and high-Ti groups of picrites can also be separated by Cr-spinel chemical compositions (Fig. 5). Cr-spinel crystals in the high-Ti picrites have higher TiO_2 at a given Al_2O_3 content (Fig. 5a), and show higher $Cr^{\#}$ and lower $Mg^{\#}$ than those in the low-Ti picrites. As a result, these two groups of picrites can be clearly distinguished from each other using the Cr-spinel compositional indicator 10Ti/Al of 0.5 (Fig. 5b). In contrast, if the classification of Kamenetsky et al. (2012) is adapted, compositional overlaps for Cr-spinel are present between some intermediate-Ti picrites and the high-Ti or low-Ti picrites. Considering the different results, we decide to use the classification of Xu et al. (2001) hereafter. Accordingly, the picrite samples from Yumen, Maoniuping, Tanglanghe and Wuguijing all belong to the high-Ti group, whereas those from Wulongba belong to the low-Ti group.

4.3. Olivine chemical compositions

As described previously by Li et al. (2012), olivine phenocrysts in the Emeishan picrites are commonly zoned, with a large homogeneous core and a very thin rim that is more Fe rich than the core. The core compositions of selected olivine grains from the Emeishan picrites from different locations, determined by EMPA, are provided as supplementary data (Table A4). Olivine phenocrysts contain 80–92 mol% Fo (100 Mg/(Mg + Fe), molar), 2000–3700 ppm Ni, 700–1700 ppm Mn, and 1400–2800 ppm Ca, and show positive Ni-Fo correlations, negative Mn-Fo correlations and no correlations between Ca and Fo (not shown), respectively. The concentrations of some trace elements in the cores of the selected olivine grains, determined by LA-ICP-MS, are provided as supplementary data (Table A5). Like the Cr-spinel compositions, olivine phenocrysts from the Yumen, Maoniuping, Tanglanghe and Wuguijing picrites contain higher Ti and lower Al contents than those from the Wulongba picrites (Fig. 5c). The olivine compositional indicator 10Ti/Al of 0.9 also can be used to divide high-Ti and low-Ti groups (Fig. 5d).

As previously reported for olivine phenocrysts in other picrite occurrences in the Emeishan flood basalt province (Yu et al., 2017), our selected grains from Yumen and other localities also plot between the fields of a pyroxenite mantle source and a peridotite mantle source that were proposed by Sobolev et al. (2007). This distinction was based on 100Ni/Mg, 100Mn/Fe and 100Ca/Fe variations in olivine (Fig. 6a, b). The Mg-Fe-Ni-Mn-Ca systematics in olivine show no significant difference between the high-Ti and low-Ti groups of picrites for the Emeishan flood basalt province. Moreover, the Mn/Zn and 10000Zn/Fe ratios in olivine phenocrysts from high-Ti picrites (Yumen, Maoniuping, Tanglanghe and Wuguijing) are similar to those of low-Ti picrites (Wulongba) and on discrimination diagrams both plot away from a pyroxenite mantle source, but entirely within the field for a peridotite mantle source (Fig. 6c, d).

4.4. Olivine oxygen isotope ratios

The oxygen isotope ratios of selected olivine phenocrysts in the Yumen high-Ti picrites, determined in situ by SIMS, are listed in Table A6. The olivine $\delta^{18}O$ values for the Yumen high-Ti picrites are from 4.7 to 5.7‰, which tend to be slightly lower than the values for the Wulongba low-Ti picrites but similar to the ranges for the high-Ti picrites elsewhere in the Emeishan flood basalts province (Fig. 7a). Olivine phenocrysts of the Yumen high-Ti picrites do not show any correlation between $\delta^{18}O$ values and Fo contents (Fig. 7a). The limited variation of olivine O isotopic compositions found in Yumen picrites is within analytical error. The mean $\delta^{18}O$ value for the olivine grains from Yumen is 5.19 ± 0.25‰ (1σ, $n = 35$), which is within the range of typical mantle olivine ($\delta^{18}O$ = 4.8–5.4‰, Mattey et al., 1994) (Fig. 7b).

The comparisons of olivine $\delta^{18}O$ values and the 10Ti/Al ratios of Cr-spinel and olivine for the Emeishan picrites are illustrated in Fig. 8a and b. The high-Ti picrites from Yumen tend to have higher Cr-spinel 10Ti/Al, but similar olivine 10Ti/Al relative to the same type of picrites from Maoniuping, Tanglanghe and Wuguijing. The high-Ti picrites all

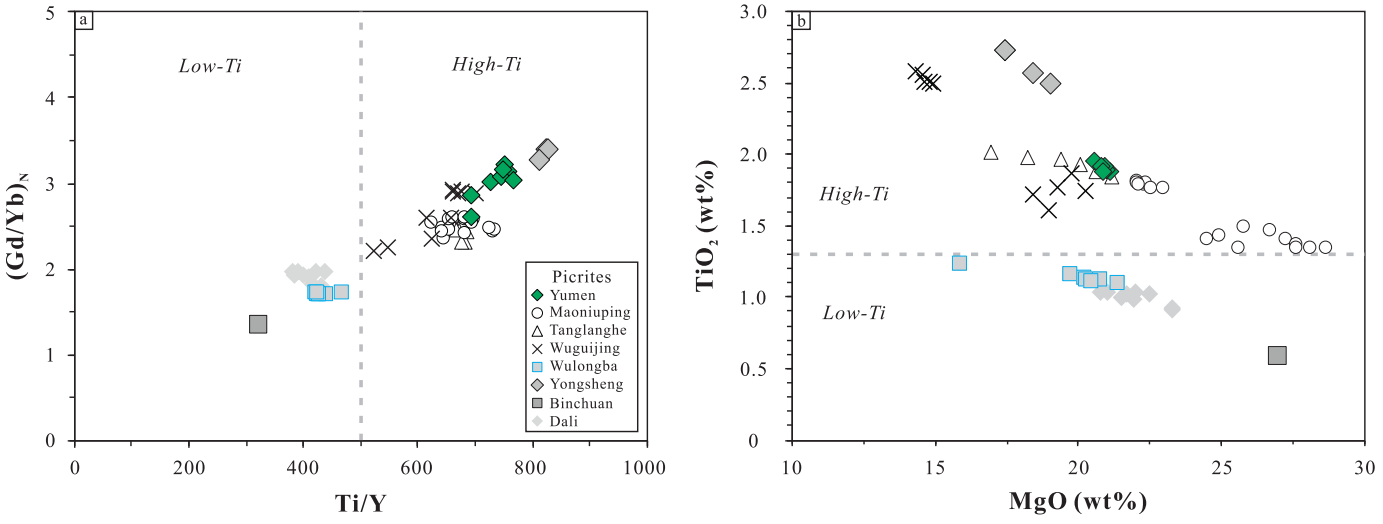

Fig. 4. Whole rock (a) Ti/Y ratios versus $(Gd/Yb)_N$ ratios (the subscript N denotes primitive mantle-normalized) and (b) MgO and Al_2O_3 contents of the Yumen picrites. The normalizing values for primitive mantle (Gd and Yb) are from Sun and McDonough (1989). The hypothetical line (Ti/Y = 500) separating high-Ti and low-Ti is from Xu et al. (2001). Data for Dali picrites are from Hanski et al. (2010). Data for Binchuan and Yongsheng picrites are from Kamenetsky et al. (2012). Data for Maoniuping, Tanglanghe, Wuguijing and Wulongba picrites are from Yu et al. (2017).

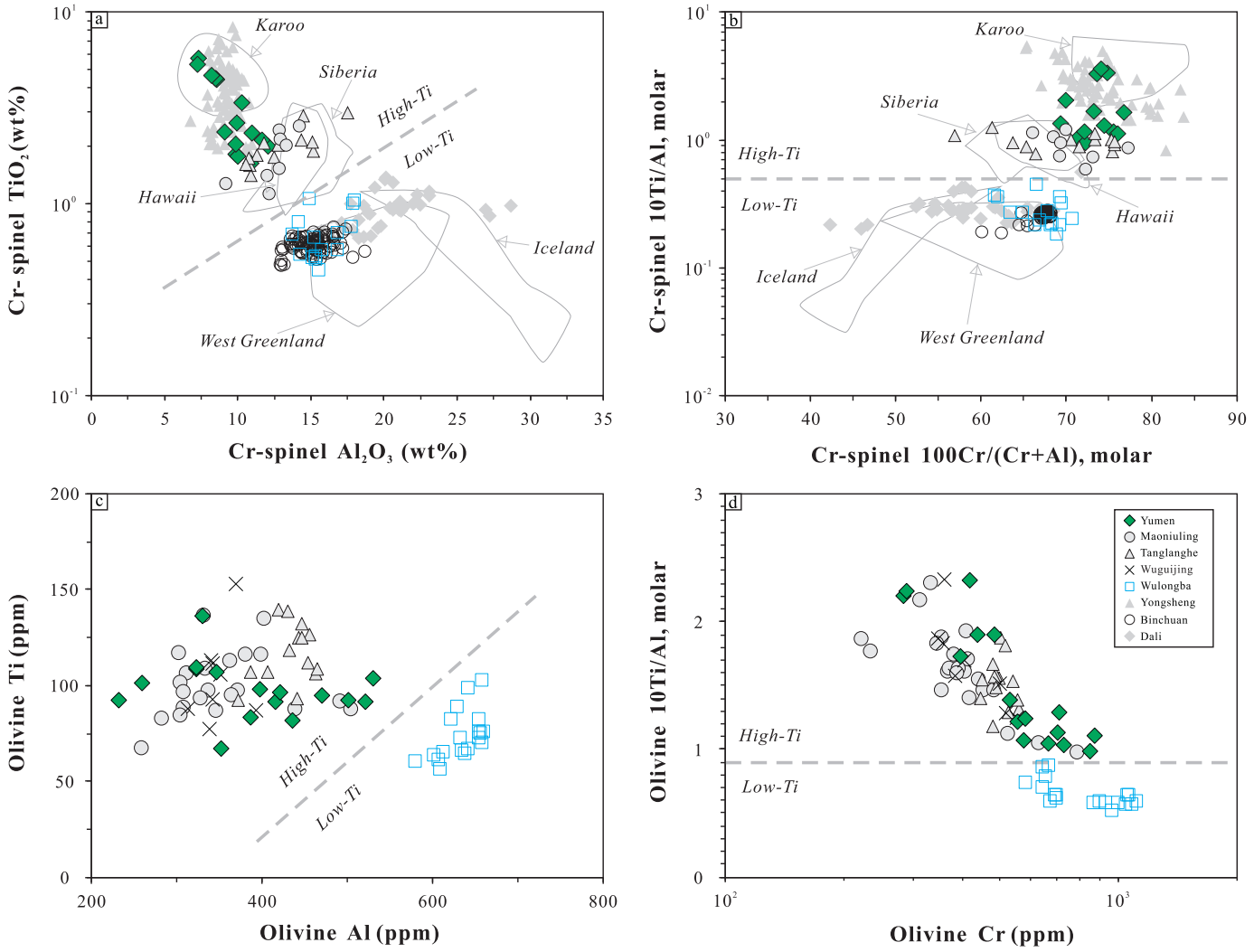

Fig. 5. (a) Al_2O_3 contents vs. TiO_2 contents, (b) (100Cr/(Cr + Al) ratios, molar) vs. (10Ti/Al ratios, molar) of Cr-spinel inclusions, (c) Al contents vs. Ti contents, and (d) Cr contents vs. (10Ti/Al ratios, molar) of olivine phenocrysts in the Emeishan picrites. The Cr-spinel data for the Dali picrites are from Hanski et al. (2010). The Cr-spinel data for the Binchuan and Yongsheng picrites are from Kamenetsky et al. (2012). Data for the fields of Karoo, Siberia, Hawaii and West Greenland and Iceland are from petrological databases (http://www.petdb.org).

have mantle-like $\delta^{18}O$ values for olivine, in contrast to the low-Ti picrites from Wolongba that have higher $\delta^{18}O$ values for olivine. The comparisons of olivine $\delta^{18}O$, Mn/Zn and 10000Zn/Fe for the Emeishan picrites are illustrated in Fig. 8c and d. There is no correlation between $\delta^{18}O$ values and Mn/Zn or 10000Zn/Fe. The element ratios of primitive olivine phenocrysts from both types of picrites in the Emeishan CFB province are all within the field for a peridotite mantle source according to the discrimination methods of Le Roux et al. (2010) and Howarth and Harris (2017).

5. Discussion

5.1. The effects of alteration, assimilation-fractional crystallization and diffusion

Partial replacement of olivine by serpentine plus secondary magnetite may have an effect on the oxygen isotope ratios of the olivine residue, mainly depending on the oxygen isotope compositions of the fluids and the prevailing temperatures (Hoefs, 2015). Bearing this in mind, we were extremely careful in grain selection. The serpentine alteration rims were commonly broken off from the fresh olivine cores during sample crushing. Those still having a visible serpentine-magnetite crust (dark) were rejected by handpicking under a microscope. Back-scattered electron images were used to select the grains that contain none or less than three micro-fractures for in situ oxygen isotope analysis. For the grains that contain one or two micro-fractures, we placed the ion beam at least 50 μm away from a micro-fracture. We have checked the possible effect of partial serpentine alteration on olivine oxygen isotope ratios by comparing the results for the grains with and without micro-fractures from the same rock sample and found no systematic variation of $\delta^{18}O$ values between these two groups of samples. Therefore, we are confident that minor serpentine alteration in the rims and in the micro-factures of the selected olivine separates did not cause significant change to the oxygen isotope ratios of the samples that we have analyzed using the in situ technique.

Assimilation-fractional crystallization (AFC) may have an effect on the oxygen isotope composition of magma and hence that of olivine crystallizing from such magma, because crustal rocks commonly have higher $\delta^{18}O$ values than primary mantle-derived magma (Hoefs, 2015). In addition to higher SiO_2 contents, crustal rocks also commonly have higher FeO/MgO contents than primary mantle-derived magma. As a result, AFC may increase olivine $\delta^{18}O$ values and decrease the Fo content of olivine. As shown in Fig. 7a, the olivine phenocrysts in the Yumen high-Ti picrites do not show any correlation between Fo contents and $\delta^{18}O$ values. This, together with the fact that the observed range of $\delta^{18}O$ values is within the range of typical mantle values given by Mattey et al. (1994), indicates that the parental magmas for the

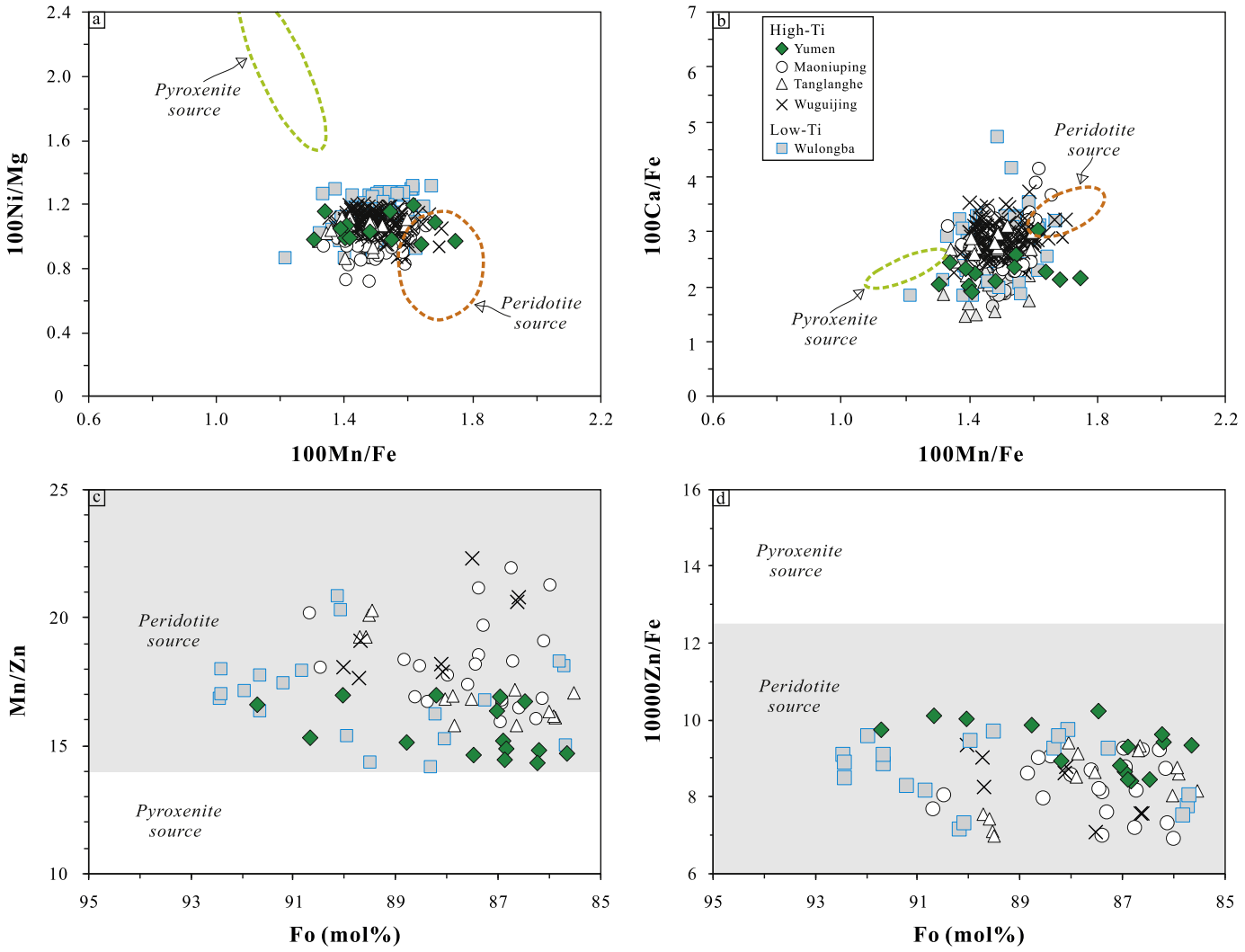

Fig. 6. (a) 100Mn/Fe vs. 100Ni/Mg ratios, and (b) 100Ca/Fe ratios, and the forsterite (Fo) contents vs. (c) Mn/Zn ratios, and (d) 10000Zn/Fe ratios of olivine from the Emeishan picrites. The fields of peridotite and pyroxenite sources in Fig. 6a and b are from Sobolev et al. (2007). The fields of pyroxenite and peridotite sourcse in Fig. 6c are from Howarth and Harris (2017). The fields of pyroxenite and peridotite sources in Fig. 6d are from Le Roux et al. (2010). Data of olivine from the Maoniuping, Tanglanghe, Wuguijing and Wulongba areas in Fig. 6a and b are from Yu et al. (2017) and this study.

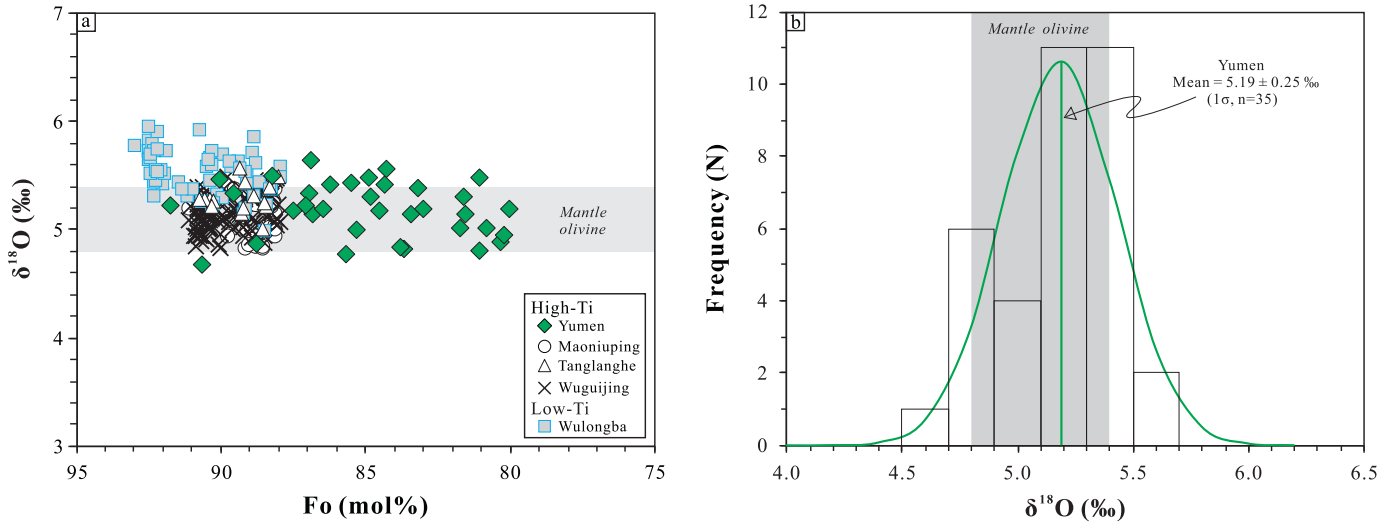

Fig. 7. Oxygen isotope composition of the olivine phenocrysts from the Yumen picrites analyzed by SIMS. (a) $\delta^{18}O$ values vs. Fo contents, (b) histogram of olivine $\delta^{18}O$ values. The dashed grey lines represent the mean $\delta^{18}O$ values of olivine from other areas. The range of $\delta^{18}O$ of olivine for mantle peridotite is +4.8 to +5.4‰, after from Mattey et al. (1994). Data of $\delta^{18}O$ values of olivine from the Maoniuping, Tanglanghe, Wuguijing and Wulongba areas are from Yu et al. (2017).

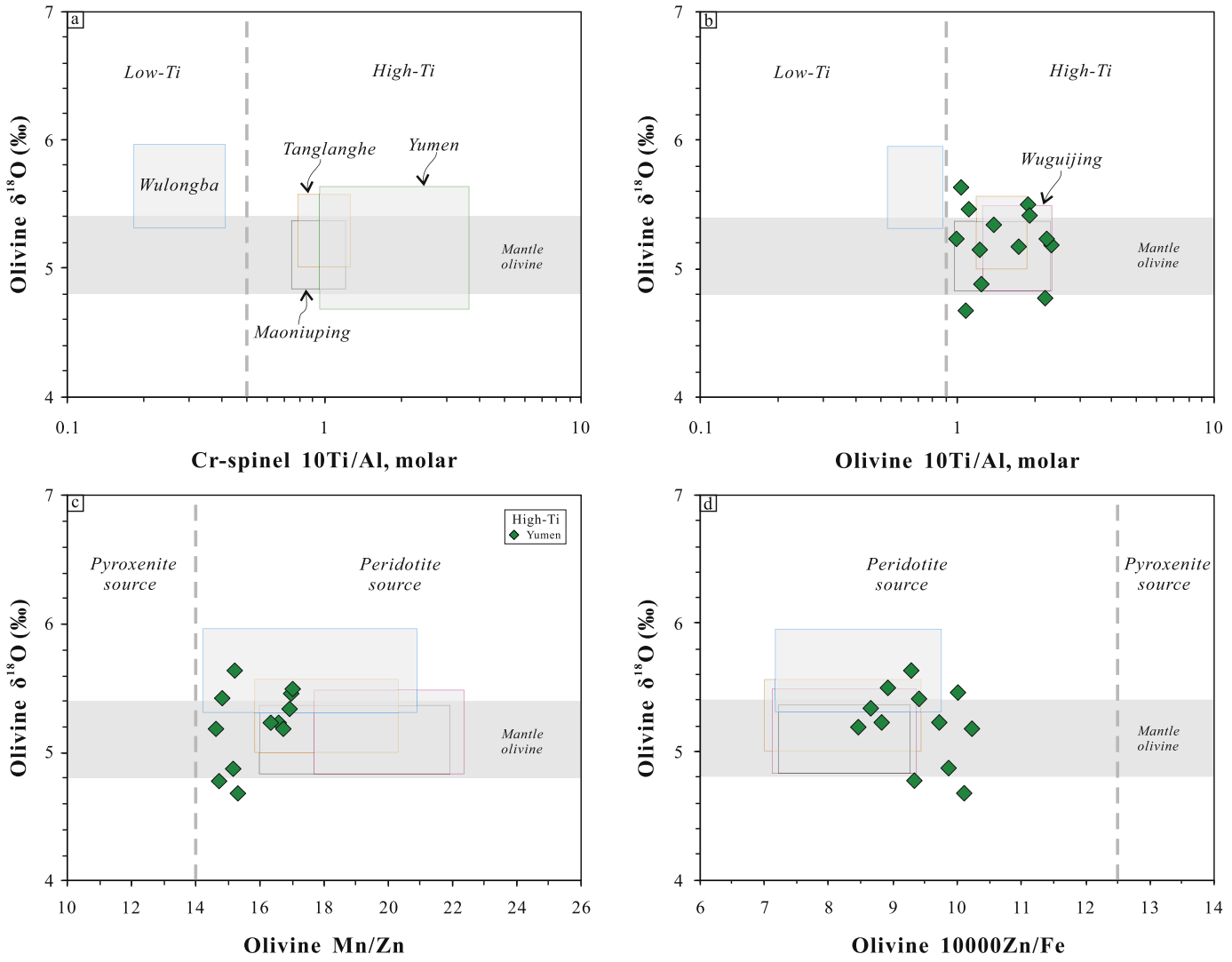

Fig. 8. Relationship between $\delta^{18}O$ values of olivine and (10Ti/Al ratios, molar) of Cr-spinel (a), and between olivine $\delta^{18}O$ values and (10Ti/Al ratios, molar) (b), Mn/Zn ratios (c), and 10000Zn/Fe (d) for the Emeishan picrites. Data of olivine $\delta^{18}O$ values for picrites from the Maoniuping, Tanglanghe, Wuguijing and Wulongba areas are from Yu et al. (2017). The fields of pyroxenite and peridotite sources are from Le Roux et al. (2010) and Howarth and Harris (2017).

selected olivine phenocrysts experienced fractional crystallization without significant crustal contamination. Oxygen isotope fractionation between olivine and picritic/tholeiitic magma is very small at magmatic temperatures (O isotopic fractionation factor $\alpha_{magma\text{-}olivine} = 1.0003$ to 1.0007; Eiler, 2001). As a result, the effect of olivine fractional crystallization on the $\delta^{18}O$ values of olivine is trivial. For example, assuming a fractionation factor of 1.0005 between olivine and magma, 10 wt% fractional crystallization of olivine from mantle-derived magma with $\delta^{18}O = 5.0‰$ only changes the $\delta^{18}O$ values by 0.05‰ for olivine, which is within analytical error. On the other hand, 10 wt% olivine fractional crystallization can cause a decrease of olivine Fo content by ~5 mol%. If the experimental K_D $[(FeO/MgO)^{olivine}/(FeO/MgO)^{melt}]$ value of 0.34 for picritic basalt (Matzen et al., 2011) is used for calculation purposes, the range of Fo contents of the selected olivine phenocrysts is similar to the result for 10 wt% fractional crystallization.

Based on an equilibrium calculation with a K_D $[(FeO/MgO)^{olivine}/(FeO/MgO)^{melt}]$ value of 0.34, the whole rock $Mg^{\#}$ (~75) of Yumen picrites is too high for a melt in equilibrium with olivine crystals that have Fo values of 80–91, suggesting the Yumen picrites should be a mixture of lava + olivine phenocrysts. The diffusion effect for O isotopes (^{18}O, ^{16}O) should be considered among olivine grains, groundmass and intracrystalline material. Bindeman (2008) proposed that a slight modification of $\delta^{18}O$ values requires a volumetrically-significant mass transformation due to oxygen being a major element. He also summarized previous experimental results for diffusion in common igneous minerals, showing that diffusion of cations (Fe, Mg, Mn, Ca and Ni) is faster than oxygen diffusion in olivine. However, almost every large olivine phenocryst in the picrites is characterized by a few microns to tens of microns thick rim with lower Fo and Ni, implying that the effects of diffusion of cations in olivine is extremely limited. In other words, the effect of oxygen diffusion on the $\delta^{18}O$ values of olivine is negligible.

5.2. Peridotite or pyroxenite mantle source for the Emeishan picrites

The mantle source composition of the Emeishan high-Ti picrites at Yumen has never been previously discussed, as this is a newly-discovered occurrence. The mantle source compositions for other high-Ti picrites in the Emeishan CFB province have been proposed. Kamenetsky et al. (2012) suggested that the high-Ti endmember (e.g. Yongsheng, see Fig. 4a) and the low-Ti endmember (e.g. Binchuan) were derived from a garnet pyroxenite source and a peridotite source, respectively, mainly based on the olivine Mg-Fe-Ni-Mn-Ca discrimination diagrams of Sobolev et al. (2007). In addition, Kamenetsky et al. (2012) suggested that both sources were situated in the lithospheric mantle instead of within a deep-seated mantle plume. Their main argument is that the whole rock Sr-Nd isotope compositions of the picrite

samples from these two different locations are very similar. Using the same olivine discrimination diagrams, plus major element compositions and Pb isotopes of melt inclusions trapped in primitive olivine phenocrysts, Ren et al. (2017) suggested that the Emeishan picrites at Yongsheng (high-Ti), Dali and Binchuan (low-Ti) were all derived from a pyroxenite-dominant source associated with a deep-seated mantle plume. In contrast, Yu et al. (2017) suggested the Emeishan high-Ti picrites at Maoniuping, Wuguijing and Tanglanghe were all derived from a peridotite-dominant mantle source containing no >20% average recycled oceanic crust, mainly because the primitive olivine phenocrysts in these samples all have $\delta^{18}O$ values that are very similar to those of typical mantle peridotites.

In the debate discussed above the olivine Mg-Fe-Mn-Ni-Ca discrimination diagrams for mantle sources proposed by Sobolev et al. (2007) have played a critical role. Those who believe in the accuracy of the discrimination diagrams tend to more strongly favor a pure pyroxenite or a pyroxenite-dominant source mantle for the picrites that show a "pyroxenite" signature in the discrimination diagrams. However, many researchers recently have warned of the use of these discrimination diagrams as conclusive evidence because the mantle source lithological variation (pyroxenites versus peridotites) is only one of many factors that may affect the Mg-Fe-Mn-Ni-Ca compositions of primitive olivine crystallizing from mantle-derived magma (Matzen et al., 2017; Niu et al., 2011, and references therein). For this reason a new and more reliable discrimination method is required to identify the mantle source characteristics of primary lava. Using the Karoo and Etendeka continental flood basalt provinces as examples, Howarth and Harris (2017) demonstrated that olivine Mn/Zn and 10000Zn/Fe give the same results as melt compositions such as FeO/MnO, Zn/Fe and (FeO/CaO-3MgO/SiO_2) for the discrimination of mantle sources. The latter are based on the results of partial melting experiments, element partitioning during partial melting and thermodynamic calculations (Herzberg, 2011; Herzberg and Asimow, 2008, 2015; Le Roux et al., 2010). As shown in the mantle source discrimination diagrams based on primitive olivine Mn/Zn and 10000Zn/Fe (Fig. 6c and d), both types of picrites in the Emeishan CFB province plot exclusively in the fields of a peridotite mantle source.

5.3. Involvement of recycled oceanic mafic crust

As described above, the Yumen high-Ti picrites contain 19.72–20.93 wt% MgO and 12.20–12.45 wt% FeO^T on LOI-free basis. At a given MgO, the Yumen high-Ti picrites tend to have slightly higher FeO^T than other picrites in the Emeishan CFB province, but have significantly (1.45–1.8 wt%) lower concentrations than the minimum value recommended for a typical ferropicrite (14 wt%, Hanski and Smolkin, 1989). Available experimental data indicate that pyroxenites and Fe-rich peridotites are the most plausible sources for magmas with compositions similar to typical ferropicrites. Based on inverse melting experiments of a Cretaceous ferropicrite containing 14 wt% FeO^T and 14 wt% MgO, Tuff et al. (2005) identified a garnet-bearing clinopyroxenite mantle source for this type of rock. Using the partial melting experimental results of Fe-rich peridotites under mantle conditions from Bertka and Holloway (1994) and Agee and Draper (2004) for comparison, Goldstein and Francis (2008) demonstrated that Archean ferropicrites, which commonly contain higher FeO^T and MgO than Phanerozoic ferropicrites, could be derived from an Fe-rich peridotite mantle source. Considering the effect of plate tectonics on mantle composition evolution, such lithologies might form through interaction of typical peridotite mantle with partial melt derived from recycled oceanic mafic crust (Sobolev et al., 2007). On one hand the experimental results favor an olivine-free pyroxenite or a Fe-rich peridotite source for the Yumen high-Ti picrites; on the other hand the Fe/Mn and Zn/Fe ratios of olivine in these picrites are inconsistent with an olivine-free pyroxenite source (Fig. 8). To reconcile these different alternatives, we propose that these picrites were derived from Fe-rich, yet still olivine-rich, lithologies, i.e., modally enriched and Fe-rich peridotites. Such lithologies could form through interaction of typical peridotite mantle with partial melt derived from recycled oceanic mafic crust (Sobolev et al., 2007).

Similarly, the causes of high Ti contents in some picrites and picritic basalts are also debated. Prytulak and Elliott (2007) suggested that high-Ti ocean island basalts cannot be produced by partial melting of a typical peridotite mantle source without the addition of recycled oceanic mafic crust in the source or assimilation of the overlying oceanic crust during magma ascent. Davis (2012) suggested that <5 wt% of recycled mafic crust in the mantle source may be needed for the generation of high-Ti ocean island basalts. Thus, it is possible that recycled oceanic crust was involved in the generation of the Emeishan high-Ti picrites by transferring a typical peridotite mantle source into a modally enriched and Fe-rich peridotite source as described above.

5.4. Implication for plume-lithosphere interaction based on low-Ti picrites

Low-Ti picrites are also common in the Emeishan CFB province but to date only the samples from Wulongba have been analyzed for olivine O isotope ratios ($^{18}O/^{16}O$, Yu et al., 2017) and Zn-Mn-Fe compositions (this study). Yu et al. (2017) suggested that the Wulongba low-Ti picrites, which have elevated $\delta^{18}O$ values for primitive olivine phenocrysts (Fig. 7a), were derived from a metasomatized lithospheric mantle overlying a deep-seated mantle plume, although a pyroxenite mantle source has also been proposed for the same type of picrites that occur elsewhere in the Emeishan CFB province based on olivine Mg-Fe-Mn-Ni systematics (e.g., Kamenetsky et al., 2012; Ren et al., 2017). Since our new olivine trace element data are consistent with a peridotite mantle source for the low-Ti picrites from Wulongba, we concur with the view of Yu et al. (2017) that these picrites were derived from a lithospheric peridotite mantle source above a mantle plume. These authors also suggested that the mantle source of the Wulongba low-Ti pircites was likely modified by previous subduction processes, because the $\delta^{18}O$ values of the most primitive olivine phenocrysts (Fo 88–91) in the samples are elevated (5.6 ± 0.15‰) as compared to the mantle values (4.8–5.4‰, Mattey et al., 1994).

5.5. A simplified petrogenic model

Based on the results from this study, we conclude that a mantle plume and the overlying lithospheric mantle were involved in the generation of the Emeishan picrites with compositions varying from low-Ti to high-Ti varieties. This is illustrated in Fig. 9. Partial melting in the ascending deep-seated peridotite-dominant mantle plume is attributed to

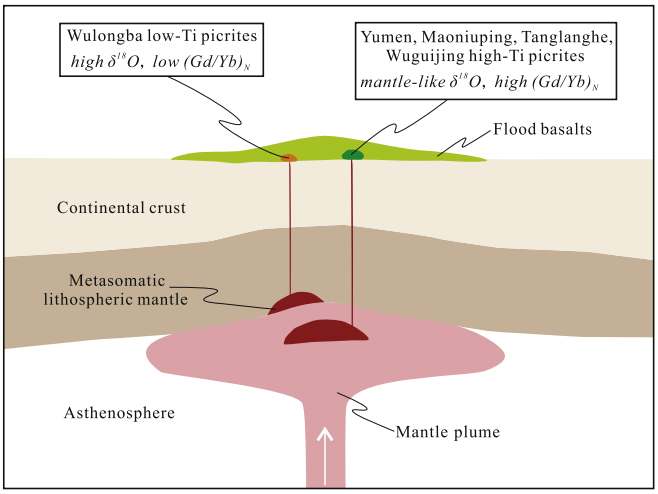

Fig. 9. Schematic diagram showing the suggested mantle sources for the studied picrites of the Emeishan flood basalt province in SW China.

associated decompression; partial melting in the overlying lithospheric peridotite mantle is attributed to conductive heat transfer from the underlying hotter plume head. The proposed depth variation between the low-Ti and high-Ti picrites shown in this model (Fig. 9) is consistent with the whole rock $(Gd/Yb)_N$ (Fig. 4a), which generally increases with the depth of partial melting. A lithospheric peridotite mantle source for the low-Ti variety is also consistent with the view of Shellnutt and Pham (2018) that is mainly based on the estimated mantle potential temperatures for low-Ti basalts that occur elsewhere in the Emeishan CFB province.

6. Conclusions

(1) The 10Ti/Al (molar) ratios of primitive olivine phenocrysts and Cr-spinel inclusions enclosed in olivine can be used to effectively distinguish between high-Ti and low-Ti picrites in the Emeishan CFB province.
(2) The Mn/Zn and 10000Zn/Fe ratios of primitive olivine phenocrysts in the studied Emeishan picrites are consistent with a peridotite mantle source for the parental magmas of these rocks.
(3) Like other high-Ti picrites in the Emeishan CFB province, the mean $\delta^{18}O$ value of the primitive olivine phenocrysts from the high-Ti picrites at Yumen is within the range of typical mantle olivine worldwide.
(4) Based on these results, we conclude that the high-Ti picrites in the Emeishan CFB province were derived from a deep-seated mantle plume developed within primarily peridotites.

Supplementary data to this article can be found online at https://doi.org/10.1016/j.lithos.2019.04.019.

Acknowledgments

This work is supported by the Chinese Academy of Sciences (Grant No.XDB18030204), the National Science Foundation of China (Grants 41425011, 41572074, and 41273049) and the National Key Research and Development Program of China (2016YFC0600502). We thank Juan Wang for his assistance in olivine chemical analysis by EMPA, Jing Hu, Guangping Bao and Yan Huang for their assistances in whole-rock chemical analysis by ICP-MS, Zhihui Dai for his assistance in olivine trace element analysis by LA-ICP-MS, and Jiao Li for his help in olivine O isotope analysis by SIMS. Constructive reviews from Profs. Greg Shellnutt and Zhaochong Zhang, and insightful inputs from the editor, have improved the quality of this paper significantly.

References

Agee, C.B., Draper, D.S., 2004. Experimental constraints on the origin of Martian meteorites and the composition of the Martian mantle. Earth Planet. Sci. Lett. 224, 415–429.
Ali, J.R., Thompson, G.M., Zhou, M.-F., Song, X.Y., 2005. Emeishan large igneous province, SW China. Lithos 79, 475–489.
Arndt, N., Chauvel, C., Czamanske, G., Fedorenko, V., 1998. Two mantle sources, two plumbing systems: tholeiitic and alkaline magmatism of the Maymecha River basin, Siberian flood volcanic province. Contrib. Mineral. Petrol. 133, 297–313.
Bertka, C.M., Holloway, J.R., 1994. Anhydrous partial melting of an iron-rich mantle II: primary melt compositions at 15 kbar. Contrib. Mineral. Petrol. 115, 323–338.
Bindeman, I., 2008. Oxygen isotopes in mantle and crustal magmas as revealed by single crystal analysis. Rev. Mineral. Geochem. 69, 2083–2093.
Bindeman, I., Gurenko, A., Sigmarsson, O., Chaussidon, M., 2008. Oxygen isotope heterogeneity and disequilibria of olivine crystals in large volume Holocene basalts from Iceland: evidence for magmatic digestion and erosion of Pleistocene hyaloclastites. Geochim. Cosmochim. Acta 72, 4397–4420.
Campbell, I.H., Griffiths, R.W., 1990. Implications of mantle plume structure for the evolution of flood basalts. Earth Planet. Sci. Lett. 99, 79–93.
Cawood, P.A., Wang, Y., Xu, Y., Zhao, G., 2013. Locating South China in Rodinia and Gondwana: a fragment of greater India lithosphere? Geology 41, 903–906.
Chung, S.-L., Jahn, B.-m., 1995. Plume-lithosphere interaction in generation of the Emeishan flood basalts at the Permian-Triassic boundary. Geology 23, 889–892.
Chung, S.-L., Lee, T.-Y., Lo, C.-H., Wang, P.-L., Chen, C.-Y., Yem, N.T., Hoa, T.T., Genyao, W., 1997. Intraplate extension prior to continental extrusion along the Ailao Shan-Red River shear zone. Geology 25, 311–314.
Davis, F.A., 2012. The Role of Partial Melts of Peridotite in the Formation of Oceanic Island Basalts. PhD thesis, Theses. University of Minnesota (17 pp.).
Deng, J., Wang, Q., Li, G., Santosh, M., 2014. Cenozoic tectono-magmatic and metallogenic processes in the Sanjiang region, southwestern China. Earth Sci. Rev. 138, 268–299.
Eiler, J.M., 2001. Oxygen isotope variations of basaltic lavas and upper mantle rocks. Rev. Mineral. Geochem. 43, 319–364.
Eiler, J.M., Farley, K.A., Valley, J.W., Stolper, E.M., Hauri, E.H., Craig, H., 1995. Oxygen isotope evidence against bulk recycled sediment in the mantle sources of Pitcairn Island lavas. Nature 377, 138.
Eiler, J., Stolper, E.M., McCanta, M.C., 2011. Intra-and intercrystalline oxygen isotope variations in minerals from basalts and peridotites. J. Petrol. 52, 1393–1413.
Ellam, R.M., 2006. New constraints on the petrogenesis of the Nuanetsi picrite basalts from Pb and Hf isotope data. Earth Planet. Sci. Lett. 245, 153–161.
Fan, W., Zhang, C., Wang, Y., Guo, F., Peng, T., 2008. Geochronology and geochemistry of Permian basalts in western Guangxi Province, Southwest China: evidence for plume-lithosphere interaction. Lithos 102, 218–236.
Goldstein, S.B., Francis, D., 2008. The petrogenesis and mantle source of Archaean ferropicrites from the Western Superior Province, Ontario, Canada. J. Petrol. 49, 1729–1753.
Gurenko, A.A., Bindeman, I.N., Chaussidon, M., 2011. Oxygen isotope heterogeneity of the mantle beneath the Canary Islands: insights from olivine phenocrysts. Contrib. Mineral. Petrol. 162, 349–363.
Hanski, E.J., Smolkin, V.F., 1989. Pechenga ferropicrites and other early Proterozoic picrites in the eastern part of the Baltic Shield. Precambrian Res. 45, 63–82.
Hanski, E., Kamenetsky, V.S., Luo, Z.-Y., Xu, Y.-G., Kuzmin, D.V., 2010. Primitive magmas in the Emeishan large igneous province, southwestern China and northern Vietnam. Lithos 119, 75–90.
Harris, C., Le Roux, P., Cochrane, R., Martin, L., Duncan, A.R., Marsh, J.S., Le Roex, A.P., Class, C., 2015. The oxygen isotope composition of Karoo and Etendeka picrites: High $\delta^{18}O$ mantle or crustal contamination? Contrib. Mineral. Petrol. 170, 8.
He, B., Xu, Y.-G., Chung, S.-L., Xiao, L., Wang, Y., 2003. Sedimentary evidence for a rapid, kilometer-scale crustal doming prior to the eruption of the Emeishan flood basalts. Earth Planet. Sci. Lett. 213, 391–405.
Herzberg, C., 2011. Identification of Source Lithology in the Hawaiian and Canary Islands: Implications for Origins. J. Petrol. 52, 113–146.
Herzberg, C., Asimow, P.D., 2008. Petrology of some oceanic island basalts: PRIMELT2. XLS software for primary magma calculation. Geochem. Geophys. Geosyst. 9. https://doi.org/10.1029/2008GC002057.
Herzberg, C., Asimow, P.D., 2015. PRIMELT3 MEGA.XLSM software for primary magma calculation: peridotite primary magma MgO contents from the liquidus to the solidus. Geochem. Geophy. Geosy. 16, 563–578.
Hoefs, J., 2015. Stable Isotope Geochemistry. Springer, Berlin.
Hou, T., Zhang, Z.C., Encarnacion, J., Santosh, M., Sun, Y.L., 2013. The role recycled oceanic crust in magmatism and metallogenesis, Os-Sr-Nd isotpes, U-Pb geochronology and geochemistry of picritic dykes in the Panzhihua giant Fe-Ti oxide deposit, Central Emeishan large igneous province. Contrib. Mineral. Petrol. 165, 805–822.
Howarth, G.H., Harris, C., 2017. Discriminating between pyroxenite and peridotite sources for continental flood basalts (CFB) in southern Africa using olivine chemistry. Earth Planet. Sci. Lett. 475, 143–151.
Ireland, T.J., Walker, R.J., Brandon, A.D., 2011. ^{186}Os–^{187}Os systematics of Hawaiian picrites revisited: New insights into Os isotopic variations in ocean island basalts. Geochim. Cosmochim. Acta 75, 4456–4475.
Jennings, E.S., Gibson, S.A., Maclennan, J., Heinonen, J.S., 2017. Deep mixing of mantle melts beneath continental flood basalt provinces: Constraints from olivine-hosted melt inclusions in primitive magmas. Geochim. Cosmochim. Acta 196, 36–57.
Jourdan, F., Bertrand, H., Blicherttoft, J., Kampunzu, A.B., 2007. Major and trace element and Sr, Nd, Hf, and Pb isotope compositions of the Karoo large Igneous Province, Botswana-imbabwe: lithosphere vs mantle plume contribution. J. Petrol. 48, 1043–1077.
Kamenetsky, V.S., Chung, S.-L., Kamenetsky, M.B., Kuzmin, D.V., 2012. Picrites from the Emeishan large Igneous Province, SW China: a compositional continuum in primitive magmas and their respective mantle sources. J. Petrol. 53, 2095–2113.
Kamenetsky, V.S., Maas, R., Kamenetsky, M.B., Yaxley, G.M., Ehrig, K., Zellmer, G.F., Bindeman, I.N., Sobolev, A.V., Kuzmin, D.V., Ivanov, A.V., 2017. Multiple mantle sources of continental magmatism: insights from "high-Ti" picrites of Karoo and other large igneous provinces. Chem. Geol. 455, 22–31.
Larsen, L.M., Pedersen, A.K., 2000. Processes in High-Mg, High-T Magmas: evidence from Olivine, Chromite and Glass in Palaeogene Picrites from West Greenland. J. Petrol. 41, 1071–1098.
Larsen, L.M., Pedersen, A.K., 2009. Petrology of the paleocene picrites and flood basalts on Disko and Nuussuaq, West Greenland. J. Petrol. 50, 1667–1711.
Lassiter, J.C., Hauri, E.H., 1998. Osmium-isotope variations in Hawaiian lavas: evidence for recycled oceanic lithosphere in the Hawaiian plume. Earth Planet. Sci. Lett. 164, 483–496.
Le Roux, V., Lee, C.-T., Turner, S., 2010. Zn/Fe systematics in mafic and ultramafic systems: Implications for detecting major element heterogeneities in the Earth's mantle. Geochim. Cosmochim. Acta 74, 2779–2796.
Li, X.-H., Li, Z.-X., Zhou, H., Liu, Y., Kinny, P.D., 2002. U–Pb zircon geochronology, geochemistry and Nd isotopic study of Neoproterozoic bimodal volcanic rocks in the Kangdian Rift of South China: implications for the initial rifting of Rodinia. Precambrian Res. 113, 135–154.
Li, X.-H., Li, Z.-X., Ge, W., Zhou, H., Li, W., Liu, Y., Wingate, M.T., 2003. Neoproterozoic granitoids in South China: crustal melting above a mantle plume at ca.825 Ma? Precambrian Res. 122, 45–83.
Li, X.-H., Li, W., Li, Q., Wang, X., Liu, Y., Yang, Y., 2010. Petrogenesis and tectonic significance of the 850 Ma Gangbian alkaline complex in South China, evidence from *in situ* zircon U–Pb dating, Hf–O isotopes and whole-rock geochemistry. Lithos 114, 1–15.

Li, C., Tao, Y., Qi, L., Ripley, E.M., 2012. Controls on PGE fractionation in the Emeishan picrites and basalts: constraints from integrated lithophile–siderophile elements and Sr–Nd isotopes. Geochim. Cosmochim. Acta 90, 12–32.
Li, C., Ripley, E.M., Tao, Y., Hu, R., 2016. The significance of PGE variations with Sr–Nd isotopes and lithophile elements in the Emeishan flood basalt province from SW China to northern Vietnam. Lithos 248, 1–11.
Liu, Y., Hu, Z., Gao, S., Günther, D., Xu, J., Gao, C., Chen, H., 2008. In situ analysis of major and trace elements of anhydrous minerals by LA-ICP-MS without applying an internal standard. Chem. Geol. 257, 34–43.
Mattey, D., Lowry, D., Macpherson, C., 1994. Oxygen isotope composition of mantle peridotite. Earth Planet. Sci. Lett. 128, 231–241.
Matzen, A.K., Baker, M.B., Beckett, J.R., Stolper, E.M., 2011. Fe–Mg partitioning between olivine and high-magnesian melts and the nature of Hawaiian parental liquids. J. Petrol. 52, 1243–1263.
Matzen, A.K., Wood, B.J., Baker, M.B., Stolper, E.M., 2017. The roles of pyroxenite and peridotite in the mantle sources of oceanic basalts. Nat. Geosci. 10, 530.
Morgan, W.J., 1971. Convection Plumes in the lower Mantle. Nature 230, 42–43.
Niu, Y., Wilson, M., Humphreys, E.R., O'hara, M.J., 2011. The origin of intra-plate ocean island basalts (OIB): the lid effect and its geodynamic implications. J. Petrol. 52, 1443–1468.
Prytulak, J., Elliott, T., 2007. TiO_2 enrichment in ocean island basalts. Earth Planet. Sci. Lett. 263, 388–403.
Ren, Z.-Y., Wu, Y.-D., Zhang, L., Nichols, A.R., Hong, L.-B., Zhang, Y.-H., Zhang, Y., Liu, J.-Q., Xu, Y.-G., 2017. Primary magmas and mantle sources of Emeishan basalts constrained from major element, trace element and Pb isotope compositions of olivine-hosted melt inclusions. Geochim. Cosmochim. Acta 208, 63–85.
Richards, M.A., Duncan, R.A., Courtillot, V.E., 1989. Flood Basalts and Hot-Spot Tracks: Plume Heads and Tails. Science 246, 103–107.
Schaefer, B.F., Parkinson, I.J., Hawkesworth, C.J., 2000. Deep mantle plume osmium isotope signature from West Greenland Tertiary picrites. Earth Planet. Sci. Lett. 175, 105–118.
Shellnutt, J.G., 2014. The Emeishan large igneous province: a synthesis. Geosci. Front. 5, 369–394.
Shellnutt, J.G., Pham, T.T., 2018. Mantle potential temperature estimates and primary melt compositions of the Low-Ti Emeishan flood basalt. Front. Earth Sci. 6, 67. https://doi.org/10.3389/feart.2018.00067.
Shellnutt, J.G., Wang, K.-L., Zellmer, G.F., Iizuka, Y., Jahn, B.-M., Pang, K.-N., Qi, L., Zhou, M.-F., 2011. Three Fe-Ti oxide ore-bearing gabbro-granitoid complexes in the Panxi region of the Permian Emeishan large igneous province, SW China. Am. J. Sci. 311, 773–812.
Shellnutt, J.G., Denyszyn, S.W., Mundil, R., 2012. Precise age determination of mafic and felsic intrusive rocks from the Permian Emeishan large igneous province (SW China). Gondw. Res. 22, 118–126.
Sobolev, A.V., Hofmann, A.W., Kuzmin, D.V., Yaxley, G.M., Arndt, N.T., Chung, S.-L., Danyushevsky, L.V., Elliott, T., Frey, F.A., Garcia, M.O., 2007. The amount of recycled crust in sources of mantle-derived melts. Science 316, 412–417.
Song, X.-Y., Zhou, M.-F., Tao, Y., Xiao, J.-F., 2008. Controls on the metal compositions of magmatic sulfide deposits in the Emeishan large igneous province, SW China. Chem. Geol. 253, 38–49.
Starkey, N.A., Stuart, F.M., Ellam, R.M., Fitton, J.G., Basu, S., Larsen, L.M., 2009. Helium isotopes in early Iceland plume picrites: Constraints on the composition of high $^3He/^4He$ mantle. Earth Planet. Sci. Lett. 277, 91–100.
Sun, S.-S., McDonough, W.-s., 1989. Chemical and isotopic systematics of oceanic basalts: implications for mantle composition and processes. Geol. Soc. Lond. Spec. Publ. 42, 313–345.
Tuff, J., Takahashi, E., Gibson, S., 2005. Experimental constraints on the role of garnet pyroxenite in the genesis of high[HYPHEN]Fe mantle plume derived melts. J. Petrol. 46, 2023–2058.
Wang, C.Y., Zhou, M.-F., Keays, R.R., 2006. Geochemical constraints on the origin of the Permian Baimazhai mafic–ultramafic intrusion, SW China. Contrib. Mineral. Petrol. 152, 309–321.
Wang, M., Zhang, Z.C., Encarnacion, J., Hou, T., Luo, W.J., 2012. Geochronology and geochemistry of the Nantianwan mafic-ultramafic complex, Emeishan large igneous province, constraints on the metallogenesis of magmatic Ni-Cu sulfide deposits and geodynamic setting. Int. Geol. Rev. 54, 1746–1764.
Xu, Y.-G., Chung, S.-L., Jahn, B.-M., Wu, G., 2001. Petrologic and geochemical constraints on the petrogenesis of Permian–Triassic Emeishan flood basalts in southwestern China. Lithos 58, 145–168.
Yao, J.-H., Zhu, W.-G., Li, C., Zhong, H., Bai, Z.-J., Ripley, E.M., Li, C., 2018. Petrogenesis and ore genesis of the lengshuiqing magmatic sulfide deposit in Southwest China: constraints from chalcophile elements (PGE, Se) and Sr-Nd-Os-S Isotopes. Econ. Geol. 113, 675–698.
Yu, S.-Y., Shen, N.-P., Song, X.-Y., Ripley, E.M., Li, C., Chen, L.-M., 2017. An integrated chemical and oxygen isotopic study of primitive olivine grains in picrites from the Emeishan large Igneous Province, SW China: evidence for oxygen isotope heterogeneity in mantle sources. Geochim. Cosmochim. Acta 215, 263–276.
Zhang, Z.C., Mahoney, J.J., Mao, J.W., Wang, F.S., 2006a. Geochemistry of picritic and associated basalt flows of the western Emeishan flood basalt province, China. J. Petrol. 47, 1997–2019.
Zhang, Z.C., Mao, J.W., Wang, F.S., Pirajno, F., 2006b. Native gold and native copper grains enclosed by olivine phenocrysts in a picrite lava of the Emeishan large igneous province. Am. Mineral. 91, 1178–1183.
Zhang, Z.C., Zhi, X.C., Chen, L.L., Saunders, A.D., Reichow, M.K., 2008. Re-Os isotopic compositions of picrites from the Emeishan flood basalt province, China. Earth Planet. Sci. Lett. 276, 30–39.
Zhang, Z.C., Mao, J.W., Saunders, A.D., Ai, Y., Li, Y., Zhao, L., 2009. Petrogenetic modeling of three mafic-ultramafic layered intrusions in the Emeishan large igneous province, SW China, based on isotopic and bulk chemical constraints. Lithos 113, 369–392.
Zhong, H., Zhu, W.-G., 2006. Geochronology of layered mafic intrusions from the Pan–Xi area in the Emeishan large igneous province, SW China. Miner. Deposita 41, 599–606.
Zhong, H., Zhou, X.-H., Zhou, M.-F., Sun, M., Liu, B.-G., 2002. Platinum-group element geochemistry of the Hongge Fe–V–Ti deposit in the Pan-Xi area, southwestern China. Miner. Deposita 37, 226–239.
Zhong, H., Campbell, I.H., Zhu, W.-G., Allen, C.M., Hu, R.-Z., Xie, L.-W., He, D.-F., 2011. Timing and source constraints on the relationship between mafic and felsic intrusions in the Emeishan large igneous province. Geochim. Cosmochim. Acta 75, 1374–1395.
Zhou, M.-F., Yan, D.-P., Kennedy, A.K., Li, Y., Ding, J., 2002. SHRIMP U–Pb zircon geochronological and geochemical evidence for Neoproterozoic arc-magmatism along the western margin of the Yangtze Block, South China. Earth Planet. Sci. Lett. 196, 51–67.
Zhou, M.-F., Robinson, P.T., Lesher, C.M., Keays, R.R., Zhang, C.-J., Malpas, J., 2005. Geochemistry, petrogenesis and metallogenesis of the Panzhihua gabbroic layered intrusion and associated Fe–Ti–V oxide deposits, Sichuan Province, SW China. J. Petrol. 46, 2253–2280.
Zhu, W.-G., Zhong, H., Li, X.-H., Deng, H.-L., He, D.-F., Wu, K.-W., Bai, Z.-J., 2008. SHRIMP zircon U–Pb geochronology, elemental, and Nd isotopic geochemistry of the Neoproterozoic mafic dykes in the Yanbian area, SW China. Precambrian Res. 164, 66–85.